SENSITIVITIES TO GEOMETRICAL AND LOADING IMPERFECTIONS ON BUCKLING OF COMPOSITE CYLINDRICAL SHELLS

Christian, HÜHNE, Rolf, ZIMMERMANN, Raimund, ROLFES, Bodo, GEIER
DLR Braunschweig, Institute of Structural Mechanics, Germany
Lilienthalplatz 7, 38108 Braunschweig, Germany
Christian.Huehne@dlr.de

ABSTRACT

Thin-walled shell structures prone to buckling are sensitive to imperfections. The influence of loading and geometrical imperfections on buckling loads of unstiffened composite cylindrical shells is investigated based on tests and computations. It is shown that their effect depends on laminate set-up. The results show that unification of imperfection sensitivity is allowed; systems sensitive to geometrical imperfections are also sensitive to loading imperfections. The results can be used to define lower limits for knock-down factors of composite shells.

1 Introduction

Imperfections can reduce the buckling load of a thin shell drastically compared to that of the perfect shell. Geometrical imperfections and loading imperfections, which influence the buckling load, are defined as deviations from perfect shape and perfect loading distributions, respectively. The ratio of nonlinear buckling loads of imperfect and perfect structures, the so-called knock-down factor, defines the sensitivity to imperfections.

Highly optimised shell structures like circular cylindrical shells are especially sensitive to imperfections, because the load is transferred by a membrane effect. Thus their consideration in the numerical simulation is essential for safe constructions. The imperfections are unknown in the design phase in general, pattern and amplitude have to be evaluated. Main focus in literature is on geometrical imperfections so far. WINTERSTETTER and SCHMIDT [1] suggest three approaches for the numerical simulation of geometrically imperfect shell structures: “realistic”, “worst” and “stimulating” geometrical imperfections. Stimulating geometrical imperfections are local perturbations which “stimulate” the characteristic physical shell buckling behaviour like weld seams [2]. “Worst” geometrical imperfections have a mathematically determined worst possible imperfection pattern like the single buckle [3]. “Realistic” geometrical imperfections are determined by measurement after fabrication and installation. The concept of measured, stochastically analysed imperfections is primarily based on the work of ARBOCZ [4]; a large number of test data is needed, which has to be classified and analysed in an imperfection data bank. Within this paper realistic geometrical imperfections, measured at test shells, are taken into account.

The investigation of different kinds of imperfections like non-uniform boundary conditions [5] or loading imperfections attracts more and more interest. Loading imperfections mean any deviations from perfect uniformly distributed loading, independent of the reason of the perturbation. GEIER, ZIMMERMANN and KLEIN tested anisotropic CFRP cylindrical shells [7], applied thin metal plates locally to perturb the applied loads and performed the so-called shim tests [8]. Later, numerical investigations were performed and compared to the test results; the importance of loading imperfections was verified [6]. The need of investigations of loading imperfections for practical use was shown for instance by ALBUS ET AL. by the example of Ariane 5 [9].

Using laminated fiber composites, the structural behaviour can be tailored by variation of fiber orientations, layer thicknesses and stacking sequence. Fixing the layer thicknesses and the number of layers, ZIMMERMANN demonstrated that variation of fiber orientations indeed affects the buckling

load remarkably [10]. Experiments corroborate these observations. The tests showed that fiber orientations can also significantly influence the sensitivity of cylindrical shells to imperfections.

In the present paper the influence of laminate set-up on sensitivity to geometrical as well as to loading imperfections is considered. The effects of geometrical and loading imperfections on the global behaviour of an unstiffened composite shell are presented and compared. Also the sensitivities of different laminate set-ups for both kinds of imperfections are investigated and compared. Since the imperfections are unknown in the design phase, an imperfection tolerant structure is desired. The feasibility of imperfection tolerant design, laminate set-up with low imperfection sensitivity combined with high buckling loads, is investigated.

In chapter 2, buckling tests are described, particularly the facility, test procedure, specimens and results. In chapter 3, the general behaviour of circular cylindrical shells with geometrical imperfections and the sensitivities of different laminate set-ups are presented. The behaviour of shells with loading imperfections and their sensitivity of their buckling loads are presented in chapter 4. Congruence of sensitivity to both, geometrical and loading imperfections, is investigated in paragraph 5, whereas conclusions are given in chapter 6.

2 Tests

2.1 Test facility and test procedure

Fig. 1 shows the test facility. The sketch illustrates the components of the test facility. The top plate is fixed during tests and reacts the force that is applied to the movable drive plate, which acts against the specimen via three load cells, a stiff load distributor and the lower end plate. Unevenness of the end plates might cause loading imperfections. In order to ensure a homogeneous loading distribution thin layers of epoxy reinforced with a mixture of sand and quartz powder (epoxy concrete) are applied between the end plates and their counterparts of the test device and are hardened under a small load. To achieve a well defined load-free state, the upper epoxy layer is separated from the top plate by a thin foil. The device is driven displacement-controlled in order to avoid damage of the test specimens.

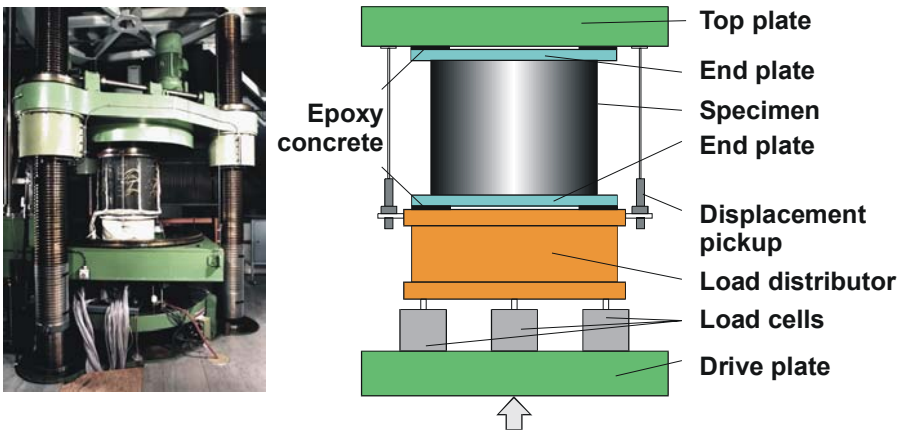

Fig. 1: Buckling test facility of DLR, Institute of Structural Mechanics

In the case of the shim tests, a thin metal plate is located between the top and the end plate, illustrated in Fig. 2. The thickness of the plate varies from t = 0.05 mm up to t = 0.4 mm. The shim is then placed in 32 predefined and equally spaced positions on the circumference, and for every position a buckling test is made and the buckling load is measured. The maximum load, which is reached before the first occurrence of a stable regular deformation pattern, is defined as buckling load. The outcome consists out of 32 values depending on the location of the shim.

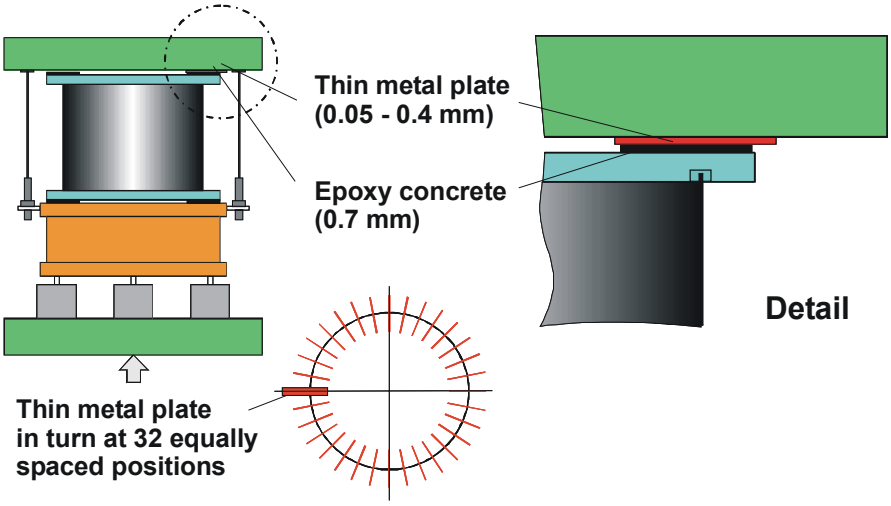

Fig. 2: Load introduction with shim tests

2.2 Test specimens

The test specimens used are listed in Fig. 3. All cylindrical shells have an inner radius of 250 mm, are composed of 4, 6, 10 unidirectional plies and are made from CFRP. The nominal ply thickness comes to 0.125 mm. The shells differ in their respective fiber orientations. The dots in the table of Fig. 3 mark the performed sets of tests. The material stiffness data of the plies are based on a large number of coupon tests and are found to be:

Modulus E_L	123550 MPa
Modulus E_T	8708 MPa
Poisson's ratio ν_{LT}	0.319
In-plane shear modulus G_{LT}	5695 MPa

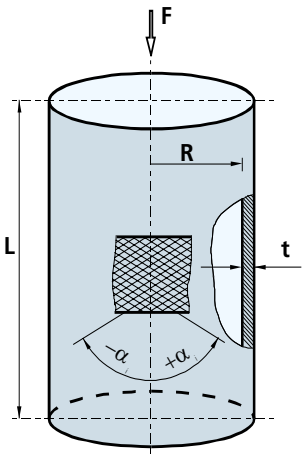

Shell No.	t_{lam} (mm)	Laminate set-up	t (mm)					
			0.00	0.05	0.10	0.20	0.30	0.40
Z26	0.5	±24/±41	•	•	•			
Z27	0.5	±75/±75	•	•	•	•	•	•
Z14	0.75	±51/90_2/±40	•		•	•		•
Z22	0.75	±49/±36/0_2	•	•	•	•		•
Z18	1.25	±37/±52/±68/0_2/±60						
Z23	1.25	±60/0_2/±68/±52/±37	•		•	•	•	•
Z24	1.25	±51/±45/±37/±19/0_2	•			•		•
Z28	1.25	±38/±68/90_2/±8/±53	•					
Z30	1.25	±30/90_2/±22/±38/±53	•					
Z33	1.25	0_2/±19/±37/±45/±51	•					

Fig. 3: Test specimens

The cylindrical shell with an original length of 530 mm is equipped with end plates to assure circular cross sections. The edges of the laminate are fitted into 10 mm deep grooves of the end plates, filled with a mixture of epoxy resin and quartz powder. By hardening of the resin the CFRP structure is bonded to the plates. The effective length of the shell becomes 510 mm [11]. The laminate set-ups of the shells are the result of an optimisation process. ZIMMERMANN [12] optimised CFRP cylindrical shells related to classical buckling load. For five ±α double layers the laminate of Z30 yields the maximum of the classical buckling load and the laminate set-up of Z24 gives the minimum of the classical buckling load. The laminates of Z23 and Z28 have buckling loads near the optimum, whereas the buckling loads of Z18 and Z33 are far away from both, maximum and minimum, of classical buckling load. For three ±α double layers Z14 has the maximum of the

classical buckling load, whereas Z22 shows the minimum. An attempt to define two laminate set-ups with similar classical buckling loads and different sensitivities to imperfections was made for Z26 and Z27 for two ±α double layers.

2.3 Test results

Several tests under uniformly distributed axial loading showed that the reduction of buckling loads depend on laminate set-up as indicated in Fig. 4. The buckling loads of different shells with identical laminate set-up 30 vary much more than those of laminate set-up 24. The shim tests, Fig. 5, made clear that the effects of loading imperfections can be influenced by laminate set-up. The reduction of buckling load of laminate set-up 23 is more severe than that of 24. An extensive evaluation of the shim tests are given in [6].

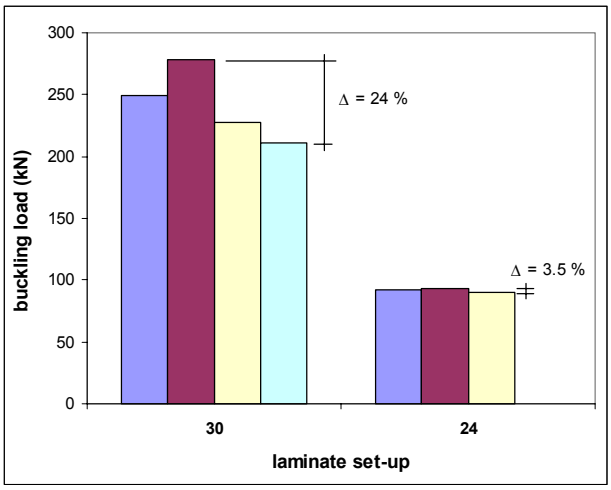

Fig. 4: Tests of axially loaded shells with uniform load introduction

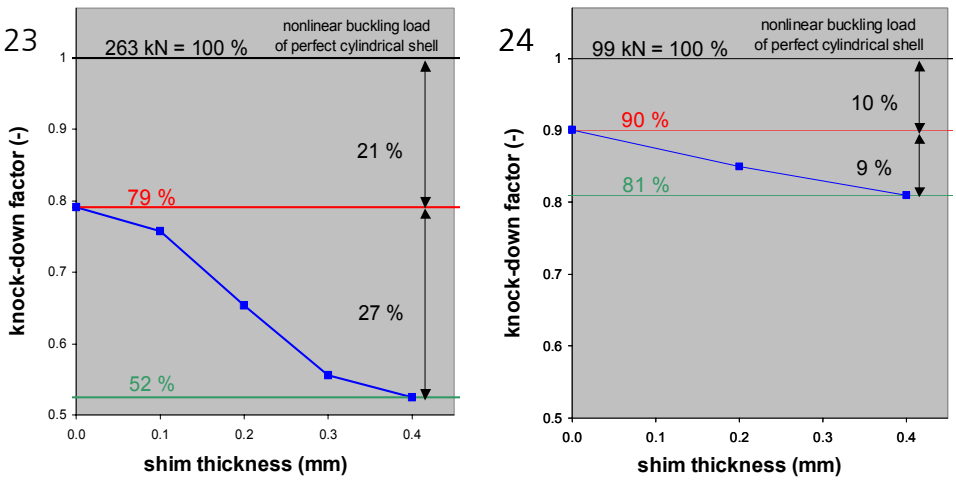

Fig. 5: Tests of axially loaded shells with non-uniform load introduction

3 Analysis of structural behaviour with geometrical imperfections

The inner surfaces of the test shells were measured with an optical sensor by EMPA [11]. Thereby 30x90 values uniformly distributed were mapped. These values were transferred to a uniformly distributed Finite Element Model which consists of 180 nodes over the circumference and 61 nodes along the length direction of the cylindrical shell. Missing values are created by linear interpolation. An developed surface of a test shell is shown in Fig. 6. On marked locations single buckles are visible. For such geometrical imperfect shells the nonlinear buckling load is determined using the Finite Element Program ABAQUS/Standard. The buckling load is defined as the maximum load, which is reached before the occurrence of a stable regular deformation pattern.

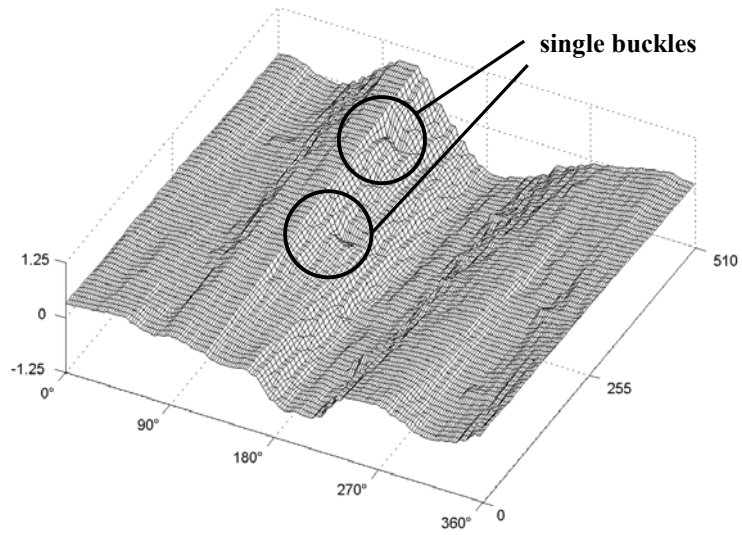

Fig. 6: Measured geometrical imperfection pattern (data given by EMPA [11])

3.1 General behaviour

The computed general structural behaviour of an unstiffened cylindrical shell under axial loading is presented in Fig. 7a-d. The deformation responses shown in the figures have been scaled for clarity. The constraint of radial displacement causes a bending boundary layer near the ends of the shell. The state of stress becomes inhomogeneous. The measured geometrical imperfections cause an additional inhomogeneous state of stress. The magnitude of this inhomogeneous state of stress and the deformations become larger with increasing load. However, the load displacement curve is nearly linear (Fig. 8). Just before buckling occurs, the shell wall deformations are characterized by one or several localized ellipse-like deformation patterns as indicated in Fig. 7a. Starting from this localized single buckle, additional local buckles have formed around the circumference at first (Fig. 7b) and then also along the length of the shell (Fig. 7c). As the buckling process continues, the deformation pattern in the shell wall continues to evolve and the ellipse-like buckles in the shell begin to conjoin into larger diamond-shaped buckles. After the kinetic energy in the shell has dissipated to a negligible level, the shell has deformed into a stable postbuckling mode-shape as indicated in Fig. 7d. The described behaviour was observed for any combination of imperfection pattern and laminate set-up and is therefore general for geometric imperfect shells.

If the axial displacement is decreased towards the initial state, the deformation pattern of diamond-shaped buckles jumps out and the stress free initial state appears. The use of linear elastic material is justified by repetition of the buckling test described before; the buckling load as well as the initial stress free state could be practically repeated about 20000 times, then repetition was stopped.

With high speed cameras it was made visible by ESSLINGER [13] that the deformation, during the transition from the initial buckling to the postbuckling state of equilibrium, starts with a single buckle. The behaviour of the calculations is very close to the behaviour observed in experiments, and the simulation of the buckling behaviour is considered to be verified.

As shown before the measured imperfection pattern includes single buckles. The single buckle is also identified as worst possible imperfection pattern [3]. The general behaviour shows that loss of stability starts with a single buckle. The single buckle is – in the terms explained before – a realistic, worst and stimulating geometrical imperfection at the same time.

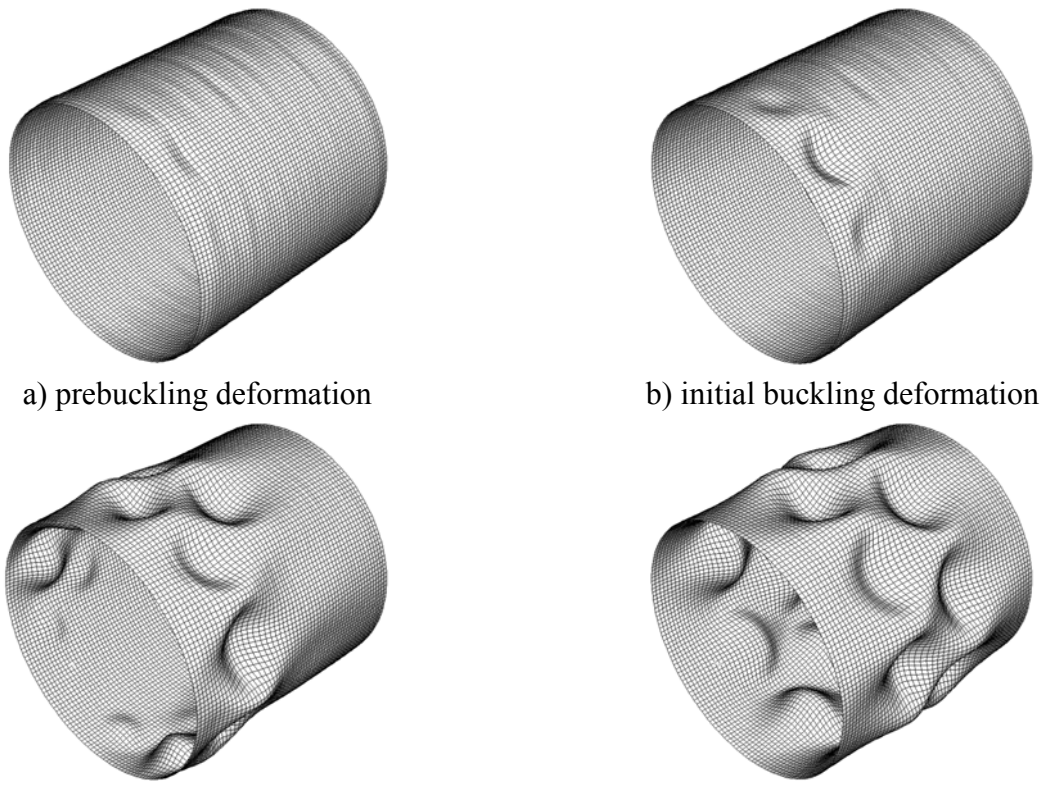

a) prebuckling deformation b) initial buckling deformation

c) transient buckling deformation d) postbuckling deformation

Fig. 7: Deformation patterns of geometrically imperfect shell

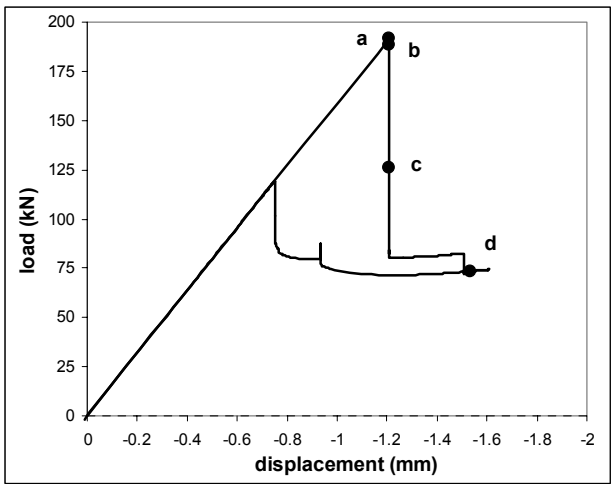

Fig. 8: Calculated load-displacement curve of geometrically imperfect cylindrical shell

3.2 Sensitivities

Six different laminate set-ups of five ±α double-layers were designed for the tests; the geometrical imperfections of eight test-shells were measured (cf. Fig. 3). The name of the imperfection agrees with the number of the associated test shell (e.g. I28). The nonlinear buckling loads are calculated for each possible combination of measured imperfection patterns and laminate set-ups. Each curve in Fig. 9a shows the nonlinear buckling load for a specific geometrical imperfection depending on the laminate set-up. The geometrical imperfection labelled with "I0" means the perfect shell; for this one the nonlinear buckling loads for laminate set-ups 23, 28, 30 are very similar, whereas the other laminate set-ups give lower buckling loads.

When coming to imperfect shells the buckling loads of the laminate set-ups 23, 28, 30 are also very similar. For imperfections I23, I31, I33 the buckling load of laminate set-up 18 is similar to these three ones. The buckling load of laminate set-up 33 is always lower than those for set-ups of 23, 28,

30 and 18. Laminate set-up 32 in any case leads to the minimum of buckling loads of investigated shells.

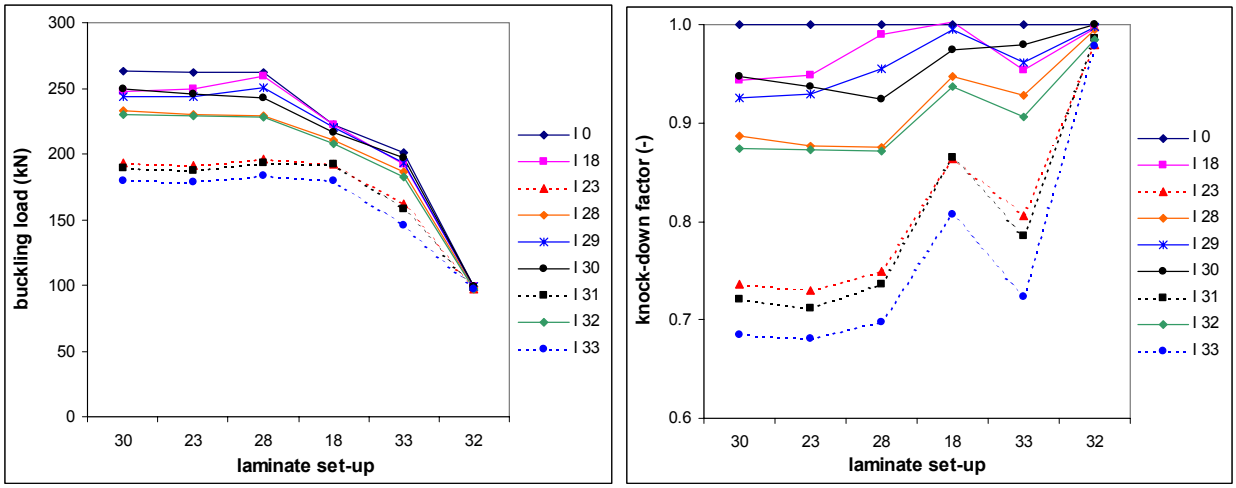

Fig. 9: Influence of geometrical imperfection pattern (I...) and laminate set-up on nonlinear buckling load (left) and knock-down factor (right)

In order to investigate the sensitivity to geometrical imperfections, the knock-down factor is calculated and shown in Fig. 9b. The knock-down factor is defined as the ratio of the buckling loads of the imperfect and the perfect cylindrical shell and quantifies the reduction of the buckling load by imperfections. Each curve in Fig. 9b is a measure for imperfection sensitivity to a specific imperfection, depending on the laminate set-up. The magnitude of the reduction depends on the geometrical imperfection. The imperfections I18, I29, I30 cause a reduction less than 10 per cent, the imperfections I28, I32 cause reductions less than 15 per cent, and the imperfections I23, I31, I33 cause reductions less then 32 per cent. The ranking of the sensitivity of different laminate set-ups is visible for different imperfections. The sensitivity of laminate set-ups 23, 28, 30 is very similar, followed by 33. Laminate set-up 18 is less sensitive and 32 is not at all sensitive to geometrical imperfections. For small geometrical imperfections (I18, I29, I30) the ranking is less significant.

Fig. 9a shows that the buckling loads of imperfect shells with different laminate set-ups can be similar although the buckling loads of the perfect shells are different. Fig. 9b makes clear that the sensitivity can be influenced by laminate set-up significantly. The results of tests in Fig. 4 corroborate these observations. The laminate set-up 18 shows that laminate set-ups with small imperfection sensitivity and high buckling load of perfect shell can be found.

4 Analysis of structural behaviour with loading imperfections

4.1 General behaviour

Shim thicknesses between 0.05 mm and 0.4 mm were used in the tests, whereas with calculations a shim thickness between 0.01 mm and 0.4 mm is simulated. For shim thickness of 0.4 mm the load-displacement curve is shown in Fig. 10. At the beginning of the deformation process the top plate is just touching the shim, no direct contact between top plate and end plate exists. When increasing the load, the end plate is pressed down and deformed at the position of the shim. The end plate is tilting. The first linear section of the load-displacement curve comes to its end when the end plate touches the top plate at the position opposite to the shim location. In the second section, the curvature part of the load-displacement curve, this opposite side of the ring is pressed down, large area contact occurs and the deformation at the position of the shim is deepened. With the third section – again a linear one – a uniformly distributed displacement of the end plate is observed until the first singular point (point a). The stiffness of the structure is higher than in the first section since large area contact between end and top plate exists.

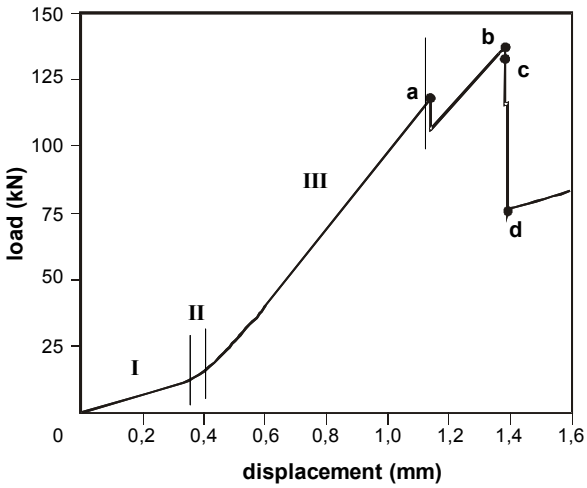

Fig. 10: Calculated load-displacement curve of cylindrical shell with loading imperfection (shim thickness 0.4 mm)

The distribution of edge forces at the top of the cylindrical shell in point a is shown in Fig. 11, a superposition of a uniform and a peak load. The integral over the peak can be interpreted as a perturbation load. The magnitude of this perturbation as well as the level of the uniform load depends on the shim thickness. The distribution of the displacement at the top of the shell is similar to the load distribution as indicated in Fig. 11.

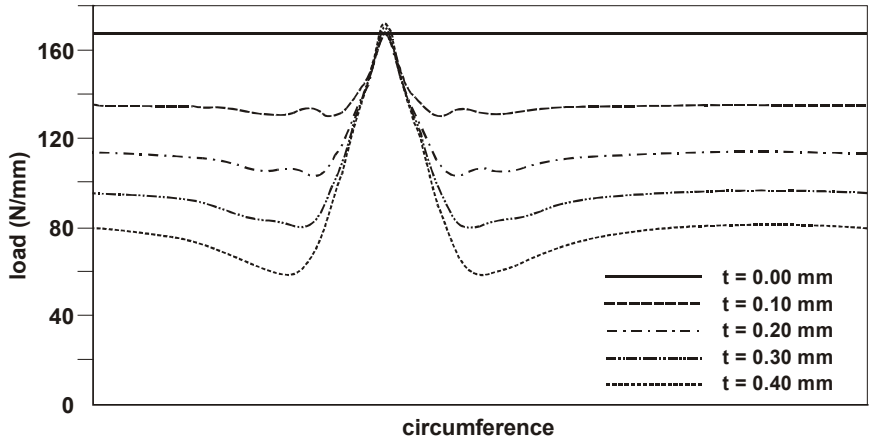

Fig. 11: Distribution of axial edge forces over circumference at upper edge of cylinder, at first singular point (point a in Fig. 10)

The implicit dynamic NEWMARK-Integration method of ABAQUS/Standard is used to calculate the load-displacement curve beyond the first singular point. For small thickness t of shims, the general behaviour there agrees with the behaviour of a geometrically imperfect shell. Starting from a local single buckle, the load decreases promptly and a stable deformation pattern of diamond-shaped buckles occurs (cf. Fig. 7 and Fig. 8). If the shim thickness becomes higher, the behaviour becomes different; the load displacement curve and deformation patterns are shown in Fig. 10 and Fig. 12, respectively. A small drop-down of the force appears just after the first singular point (point a), the local single buckle becomes deeper and moves down in axial direction. Increasing the axial displacement, the single buckle enlarges as well as the resultant axial load (point b), which becomes larger than the load at the first singular point. The axial stiffness is reduced by the local single buckle. When further increasing the displacement, starting with initial buckling behaviour (point c) the load drops off and the deformation pattern changes to one row of buckles (point d). The behaviour between the initial buckling process and the stable postbuckling deformation pattern is influenced by several numerical parameters.

The load in the first singular point is not the maximum load. Between point a and b local buckling behaviour appears whereas after passing the maximum load level, a stable regular deformation pattern occurs (point d). Therefore the load at point b is defined as the buckling load. Just as the

general behaviour of geometrically imperfect shells, the buckling process here also starts with a local single buckle.

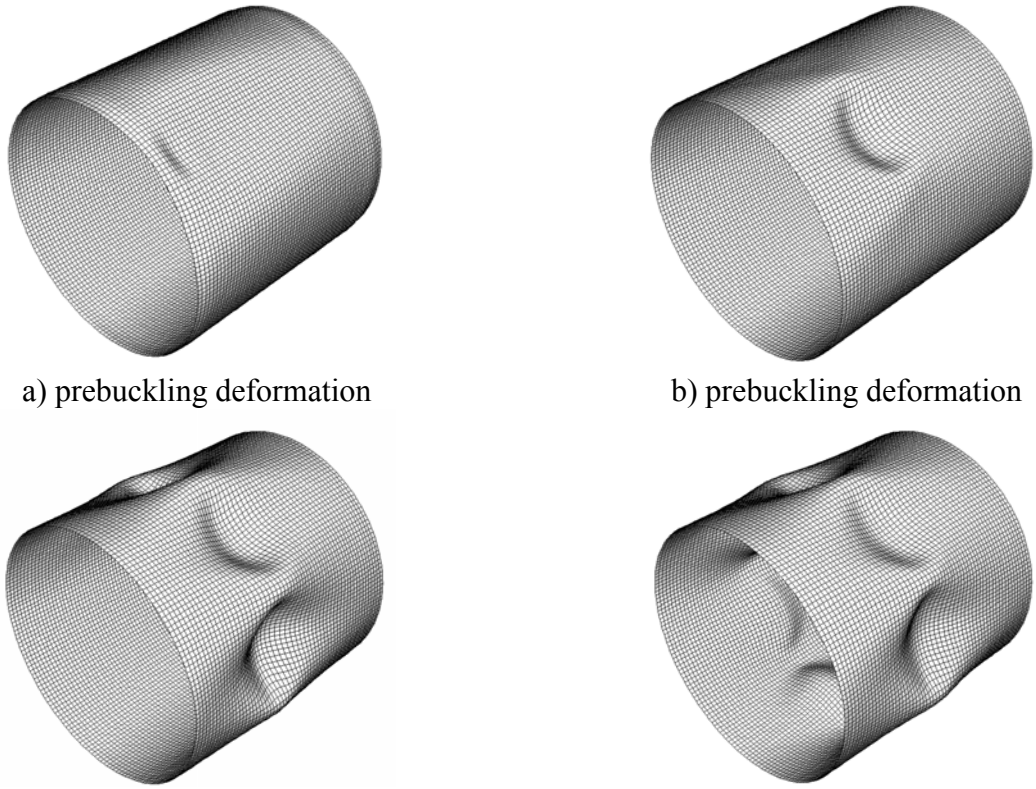

a) prebuckling deformation

b) prebuckling deformation

c) initial buckling deformation

d) postbuckling deformation

Fig. 12: Deformation patterns of shell with loading imperfections

4.2 Sensitivities

To investigate the sensitivity to loading imperfections, the nonlinear buckling load and the knock-down factor are calculated for several combinations of shim thicknesses and laminate set-ups as indicated in Fig. 13.

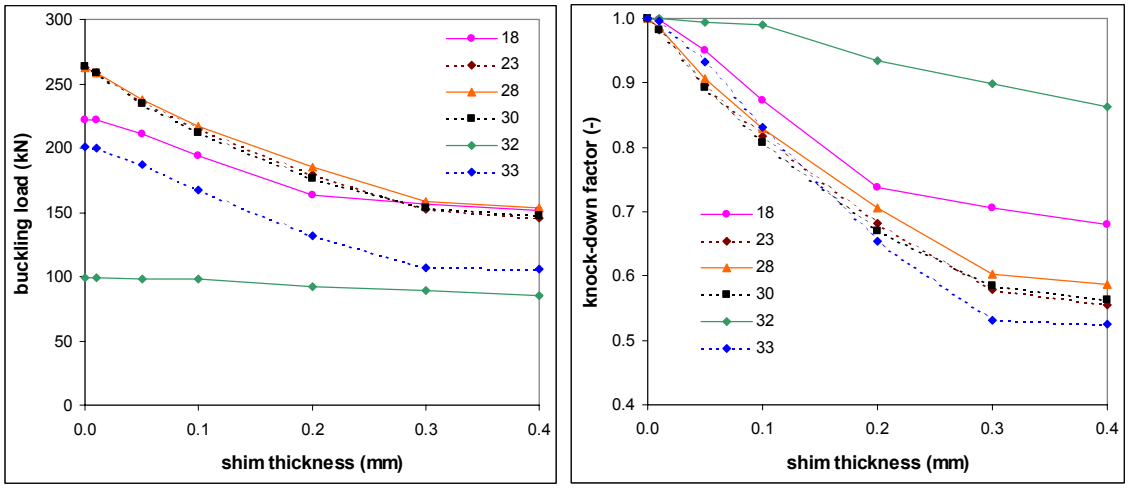

Fig. 13: Influence of loading imperfection and laminate set-up on nonlinear buckling load (left) and knock-down factor (right)

Regarding imperfect shells the buckling loads of the laminate set-ups 23, 28, 30 are also (cf. Fig. 9) very similar. The buckling load of laminate set-up 18 is lower than these three for shim thickness up to 0.2 mm. For larger shim thicknesses the buckling loads are nearly equal. The buckling loads of laminate set-ups 33 and 32 are far away from the other values. The gradient of 33 is the highest, 32 has the smallest one (cf. Fig. 13a).

The knock-down factors (cf. Fig. 13b) of the three laminate set-ups 23, 28, 30 are, just as the associated buckling loads, nearly equal. The curve of 33 crosses other curves; the ranking of sensitivity to loading imperfections depends on the magnitude of imperfection. Laminate set-up 18 is less sensitive than the others and 32 is nearly unsensitive to small loading imperfections.

As shown in Fig. 11 the shim causes a displacement at the upper boundary of the cylindrical shell which consists of a uniformly and a non-uniformly distributed part. The shape of the non-uniformly distributed part is a peak. Shape and magnitude of this part determine a perturbation energy that characterizes the imperfection. The number of variables to describe the effect of imperfections is reduced to a scalar value. The results are indicated in Fig. 14.

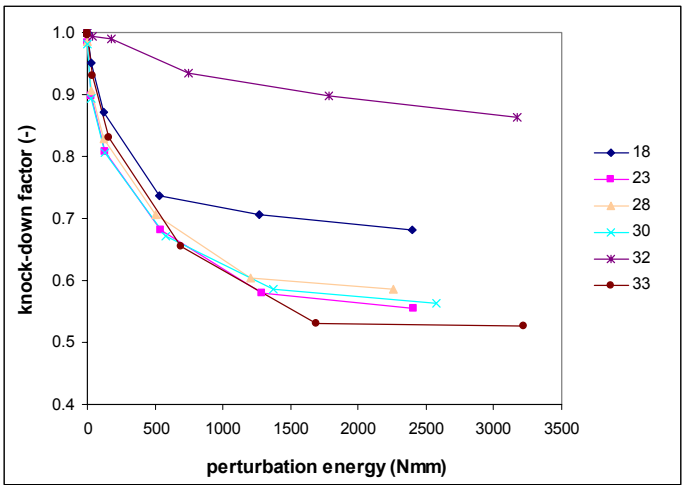

Fig. 14: Influence of loading imperfections depending on perturbation energy

The ranking of different sensitivities of laminate set-ups for a specific perturbation energy are similar to preceding investigations, Fig. 13. The results shown in Fig. 14 are used to compare geometrical and loading imperfection in the next chapter.

5 Comparison of sensitivities to geometrical and loading imperfections

Numerical investigations of the loading imperfection tests showed that the non-uniformly distributed load causes a single buckle before global buckling occurs. The similar physical effect is observed for geometrical imperfect shells. These observations allow the assumption, that the sensitivity to loading imperfections is very similar to the sensitivity to geometrical imperfections.

The results of sensitivities to loading imperfections are evaluated for a small (E=50 Nmm) and a large (E=500 Nmm) imperfection which is quantified by the energy of external forces as described before. The results are presented in comparison to geometrical imperfections in Fig. 15.

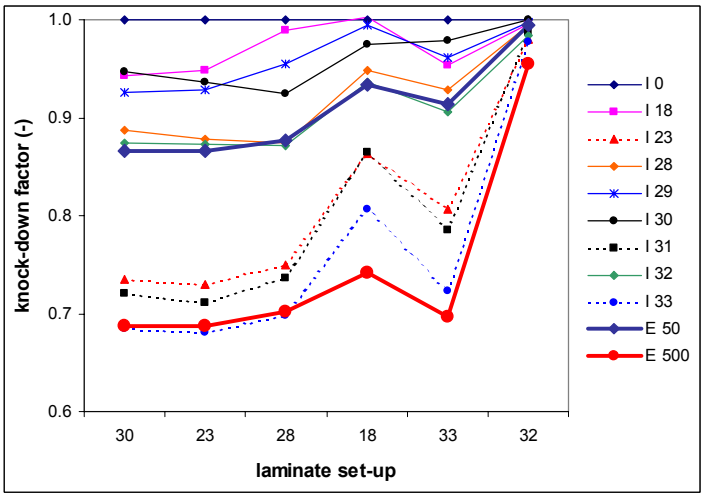

Fig. 15: Comparison of geometrical and loading imperfections

The sensitivities to geometrical and loading imperfections are nearly the same for small loading imperfections (E=50 Nmm). The quantity of reduction for small loading imperfections agrees with that of the geometrical imperfections I28 and I32.

For larger loading imperfections the quantities of reductions agree with those of geometrical imperfections of test shell 33, except laminate set-up 33 which differs more. However, the rankings of sensitivities to geometrical and loading imperfections coincide. With increase of loading imperfections sensitivities differ more from those of geometrical imperfections, because the structure reveals significantly different general behaviour compared to small imperfections, cf. sections 3.1 and 4.1. That difference causes the different shape of the load displacement curve of Fig. 8 and Fig. 10 beyond points a.

In any case, the curve for 500 Nmm energy is practically a smooth lower bound for the knock-down factors of all the laminates investigated. This observation can be used to define lower limits for knock-down factors, which depend on the specific laminate set-ups.

6 Conclusion

The loss of stability is initiated by a local single buckle. Single buckles are realistic, stimulating and worst geometrical imperfections. The buckling process of shells with loading imperfections starts also with a local single buckle. The influence of loading and geometrical imperfections on buckling loads depends on laminate set-up. The results show that unification of imperfection sensitivity is allowed; systems sensitive to geometrical imperfections are also sensitive to loading imperfections. The designer is able to trim the imperfection sensitivity and the buckling load by variation of laminate set-up. The results can be used to define lower limits for knock-down factors of composite shells.

7 References

[1] Th.A. Winterstetter and H. Schmidt, Stability of circular cylindrical steel shells under combined loading, *Thin-Walled Structures,* 40, p. 893-909, 2002

[2] M. Pircher and R. Bridge, The influence of circumferential weld-induced imperfections on the buckling of silos and tanks, *Journal of Constructional Steel Research*, 57(5), p. 569-580, 2001

[3] M. Deml and W. Wunderlich, Direct evaluation of the 'worst' imperfection shape in shell buckling, *Computer Methods in Applied Mechanics and Engineering*, 149 [1-4], p. 201-222, 1997

[4] J. Arbocz and J.H. Starnes Jr., Future directions and challenges in shell stability analysis, *Thin-Walled Structures*, 40, p. 729-754, 2002

[5] J. Arbocz, The effect of imperfect boundary conditions on the collapse behavior of anisotropic shells, *International Journal of Solids and Structures*, 37, p. 6891-6915, 2000

[6] C. Hühne, R. Zimmermann, R. Rolfes and B. Geier, Loading Imperfections – Experiments and Computations, *Euromech Colloquium 424*, 2-5 September, Kerkrade, The Netherlands, 2001

[7] B. Geier, H. Klein and R. Zimmermann, Buckling Tests with Axially Compressed Unstiffened Cylindrical Shells Made from CFRP, *Proceedings, International Colloquium on Buckling of Shell Structures*, on Land, in the Sea, and in the Air, J.F. Jullien, ed.: Elsevier Applied Sciences, London and New York, 498-507, 1991

[8] B. Geier, H. Klein, and R. Zimmermann, Experiments on Buckling of CFRP Cylindrical Shells Under Non-Uniform Axial Load, *Proceedings of International Conference on Composites Engineering*, ICCE/1 28-31 August, 1994

[9] J. Albus, J. Gomez-Garcia, and H. Oery, Control of Assembly Induced Stresses and Deformations due to the Waviness of the Interface Flanges of the ESC-A Upper Stage, 52nd *International Astronautical Congress*, 1-5 Oct 2001, Toulouse, France

[10] R. Zimmermann, *Buckling Research for Imperfection Tolerant Fiber Composite Structures*, Proc. Conference on Spacecraft Structures, Material & Mechanical Testing, Nordwijk, The Netherlands, 27-29 March, ESA SP-386, 1996

[11] H.R. Meyer-Piening, M. Farshad, B. Geier and R. Zimmermann, Buckling loads of CFRP composite cylinders under combined axial and torsion loading – experiments and computations, *Composite Structures*, 52, p. 427-435, 2001

[12] R. Zimmermann, Optimierung axial gedrückter CFK-Zylinderschalen*, Fortschrittsberichte VDI*, Nr. 207, 1992

[13] M. Esslinger, Hochgeschwindigkeitsaufnahmen vom Beulvorgang dünnwandiger, axialbelasteter Zylinder, *Der Stahlbau*, 3, 1970